Fractal characterization of the fracture surface of a high-strength low-alloy steel

J. C. HSIUNG, Y. T. CHOU
Department of Materials Science and Engineering, Lehigh University, Bethlehem, PA 18015, USA

The fractal dimension of fracture surfaces of a high-strength low-alloy steel (ASTM A710) has been measured using different ruler lengths. The fractal dimension increases with increasing impact toughness, E, and can be expressed by the quantitative relationship, $E = E_0 e^{25D'}$, where $E_0 = 1.9$ J representing the impact toughness in Euclidean space, and D' is the fractal dimensional increment, defined by $D' = D_S - 2 = D_L - 1$ and D_S and D_L are respectively, the surface and linear fractal dimensions.

1. Introduction

Irregular surfaces such as the fracture surfaces of metals, can be characterized by fractal geometry [1]. In many cases, such characterization has proved useful because the new geometry can provide a quantitative method of characterizing a fracture surface on the basis of a parameter called the surface fractal dimension, D_S.

Fractal geometry was introduced by Mandelbrot [2] to describe irregular phenomena in nature. According to Euclidean geometry, a straight line, a square, or a cube can be regarded as a one-, two-, or three-dimensional object, respectively. However, most objects in nature have contours more complicated than these simple geometrical shapes. It should not then be surprising that the dimension of a fracture surface is not an integer, as claimed by the new fractal geometry. It is further noted that the most distinct characteristic of fractal geometry is self-similarity; that is, the shape of a local part is similar to that of the whole configuration. In the case of a fracture surface, self-similarity does not hold in the strict sense but appears statistically.

The fractal dimension, which is invariant under a sufficiently small length scale and is closely linked to the concept of geometrical self-similarity, is an intrinsic property and can be used for surface characterization. Most geometrical figures in nature have a characteristic dimension to describe their shape. However, the basic relationship between material properties and fractal dimensions has yet to be explored. At present, there exists a simple relationship between the toughness and fractal dimension, i.e. the higher the fractal dimension, the tougher the material [3–5]. On the other hand, an inverse correlation has also been demonstrated by other authors [1, 6–9]. This unrealistic behaviour was later explained as the result of the use of a relatively large "ruler length" which destroys the basis of self-similarity [8].

In the present work, we intend to clarify whether fracture surfaces can be characterized by fractal geometry and to establish a correlation between the fractal dimension and impact toughness of a high-strength low-alloy steel (ASTM A710 steel). This precipitation aged, microalloyed steel is commonly used as a constructional material of high strength and toughness combined with excellent fabrication weldability [10–14].

2. Theoretical background

At present, there are a number of methods for quantitative measurement of fracture surface [1, 15, 16]. A convenient technique, known as the slit island method, was introduced by Mandelbrot *et al.* to determine the fractal dimension of a given surface [1]. This method is based on measurements of the area and perimeter of the "islands" that appear on polished sections of a fracture surface.

It is well-known that the perimeter of a Euclidean shape can be related to the surface area of the shape, usually through a simple relation. For example, the perimeter (length) of a square is equal to 4 $(\text{area})^{1/2}$. Other shapes can be shown to have the same general relationship, i.e. $(\text{length}) \propto (\text{area})^{1/2} \propto (\text{volume})^{1/3}$. Mandelbrot has given a generalized correlation between the perimeter and the area in a fractal space [2], i.e. $(\text{area})^{1\,2} \propto (\text{length})^{1/D_L}$, where D_L is the linear fractal dimension. For geometrically similar shapes, this area–length ratio is constant, leading to a unique value of D_L, which can be found by plotting the values of length and area on the log–log scale. Mathematically, we have

$$(\text{area})^{1/2} = \alpha(\text{length})^{1/D_L} \tag{1}$$

and

$$\log(\text{area}) = 2\log\alpha + (2/D_L)\log(\text{length}) \tag{2}$$

where α is a constant. Equation 2 can be used for the experimental determination of D_L on a given surface, as shown in the next section.

0022–2461

3. Experimental procedure

The material used for this investigation is ASTM A710 steel, class 3, with the composition given in Table I. Hot-rolled plates, 19 mm (0.75 in) thick, were austenized at 904 °C (1660 °F) for 1 h, water quenched, and aged at 627 °C (1160 °F) for 1 h. The microstructural constituents are primarily proeutectoid ferrite with some acicular ferrite and bainite; the average grain size is 7.1 μm. The fracture surfaces were obtained by standard Charpy impact tests conducted at various temperatures. The test specimens were machined parallel to the rolling direction.

To determine the fractal dimension of fracture surfaces of the steel, the slit island technique [1] was used. The newly separated fracture surfaces were cleaned,

TABLE I Chemical composition of A710 steel

Chemical composition (wt %)	Specified	Measured
C	0.070 max.	0.050
Mn	0.400–0.700	0.500
P	0.025 max.	0.010
S	0.025 max.	0.002
Si	0.400 max.	0.350
Ni	0.700/1.000	1.000
Cr	0.600/0.900	0.720
Mo	0.150/0.250	0.230
Cu	1.000/1.300	1.170
Nb	0.020 min.	0.032
Al	Not specified	0.018
N	Not specified	–
V	Not specified	0.003
Ti	Not specified	0.005

TABLE II Toughness of the A710 steel as a function of linear fractal dimension

Specimen no.	Temperature (°C)	Impact energy[a] (J)	D_L × 50	D_L × 500	D_L × 1250
1	− 145	9.5	1.1835	1.1213	1.0634
2	− 130	12.2	1.1579	1.1280	1.0871
3	− 110	28.5	1.1349	1.1491	1.1042
4	− 105	54.2	1.1114	1.1868	1.1287
5	− 100	126.1	1.0940	1.2106	1.1553
6	− 80	172.2	1.0717	1.2168	1.1801
7	− 60	198.0	1.1258	1.2273	1.1873
8	− 20	238.7	1.0117	1.2480	1.2009

[a] Each data point represents the average of 3–5 measurements.

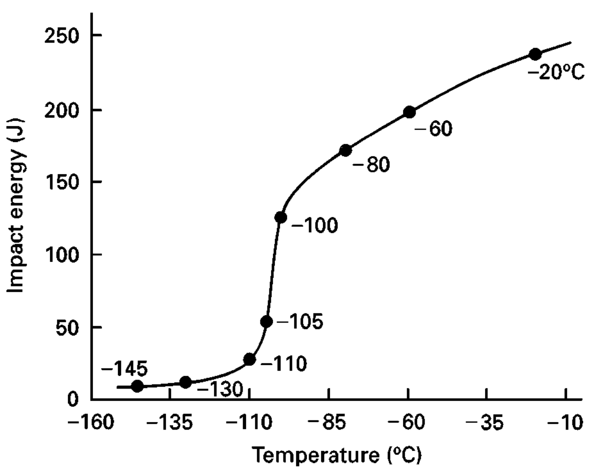

Figure 1 Charpy transition curve of A710 steel.

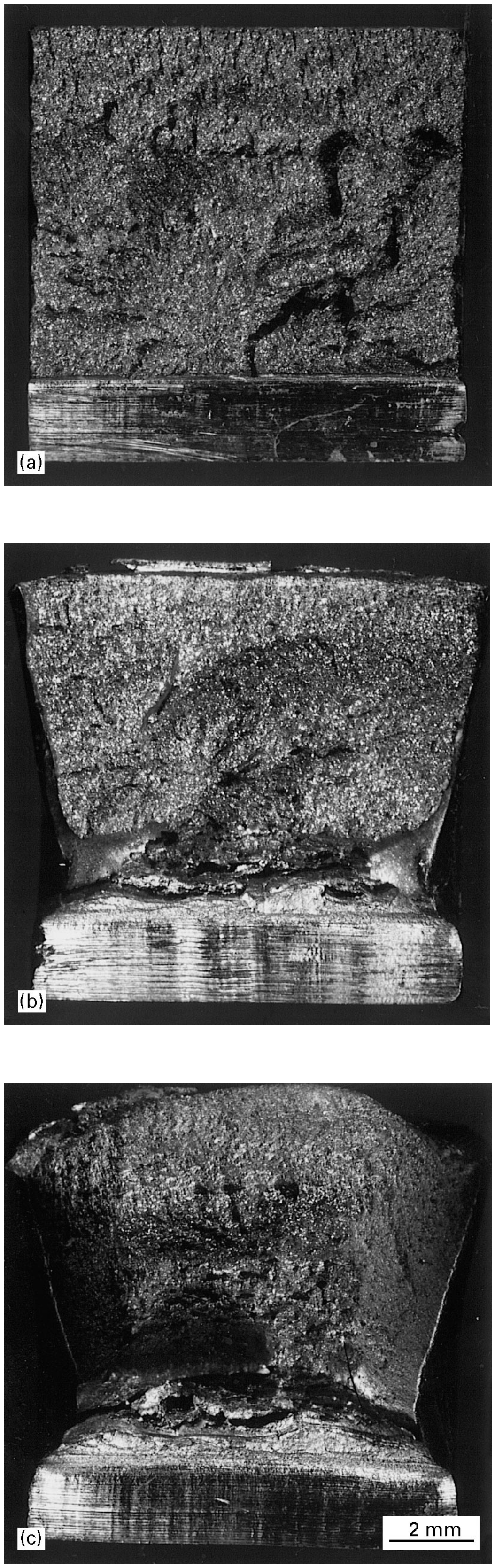

Figure 2 Fracture-mode transition in A710 steel induced by change in test temperature: (a) flat fracture at −145 °C, (b) a mixed mode of flat fracture and slant fracture at −100 °C, and (c) slant fracture at −20 °C.

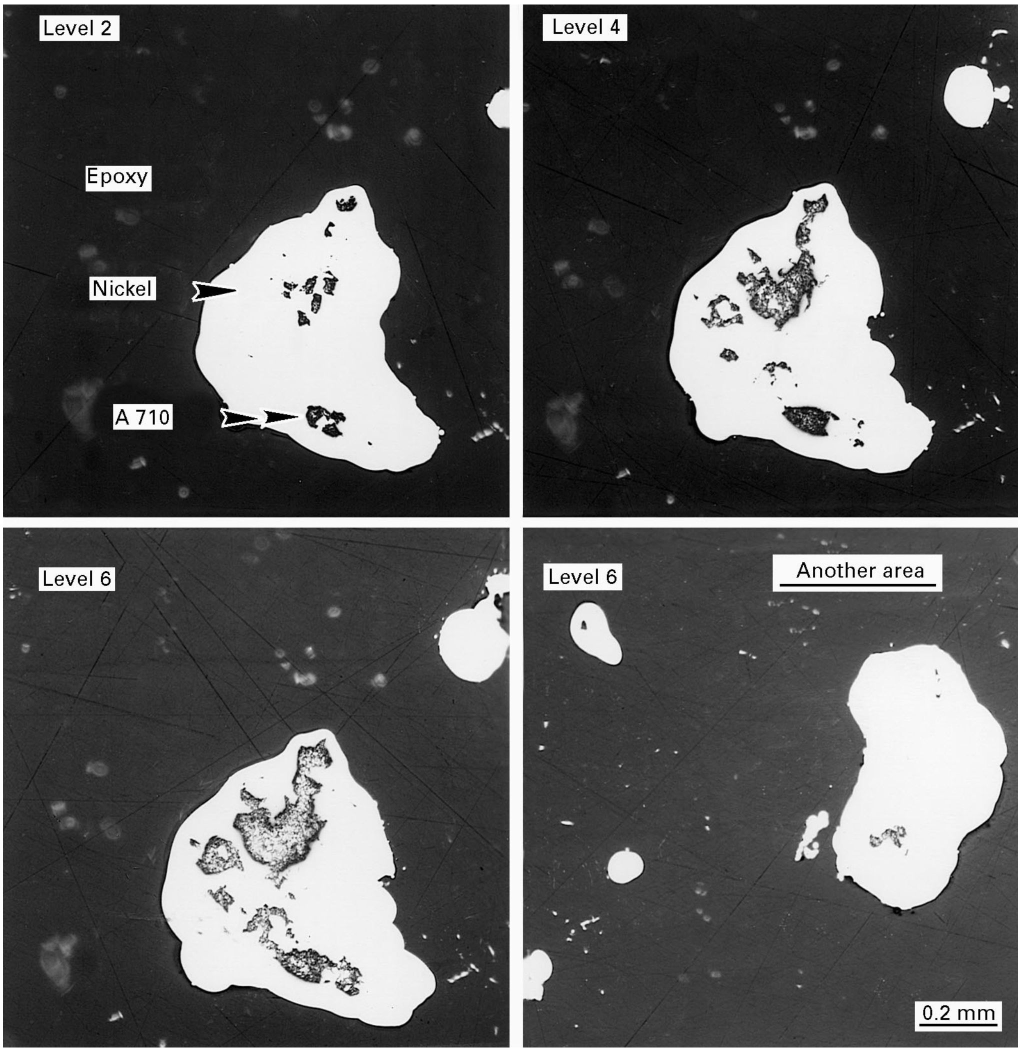

Figure 3 Optical micrographs showing the "islands" of a fracture surface at different levels.

dried, and fully coated with electroless nickel. The specimens were mounted in epoxy and then polished with 240, 320 and 400 grit papers, with the plane of polish parallel to the macroscopic plane of the fracture surface.

When the fracture surface began to appear through the semi-transparent plastic, 600 grit paper was used. As the polishing procedure progressed, the surface was checked frequently for the fracture tips of the specimen. As soon as a tip revealed, the polishing was stopped. The exposed portion of the specimen appeared as a tiny island. A set of photomicrographs was taken at $\times 50$, $\times 500$ and $\times 1250$ magnifications. For the remainder of the polishing procedure, the specimen was polished using 6 μm diamond paste. In an attempt to obtain better quality photographs, 0.3 μm Al_2O_3 and 0.05 μm SiO_2 abrasives were used for additional polishing. The specimen was then etched with 2% nital solution.

At varying intervals during polishing, each corresponding to the removal of a few micrometres, the specimen was photographed at $\times 50$, $\times 500$ and $\times 1250$. A series of 12 to 40 photographs was taken for each specimen. The progression of island growth, as well as the appearance of new islands, was shown by the consecutive series of photographs.

The photographs were analysed on a digital image analysis system (Microplan II, the Optical Apparatus Co., Inc.) by which the perimeter and area of each island were measured using a cursor to trace the enclosed curve. The magnification and the digital image pad resolution (set at 333 μm) define the scale or ruler length. From the information given by the system, one is able to derive the linear fractal dimension, D_L, of a given specimen using a log–log plot of area versus perimeter. The slope of the straight line fitted to these data points can be obtained by a linear least-square programme. The slope is equal to $2/D_L$.

4. Results and discussion

4.1. Charpy impact testing

The Charpy test results obtained for the A710 steel are shown in Table II and the transition curve in Fig. 1. As expected, the impact energy is a sigmoidal function of the testing temperature, with a transition temperature of $-105\,^{\circ}C$.

4.2. Macroscopic observation of the fracture surface

The level of fracture toughness can be related to the relative amounts of flat and slant fracture features, and the fractured surfaces of these specimens changed their morphology with the test temperature. When the fracture surface is macroscopically flat (Fig. 2a), plane-strain test conditions prevail, and the observed fracture toughness is low. If the fracture is completely of the slant or shear type (Fig. 2c), plane-stress conditions dominate to produce a tougher failure. Obviously, a mixed fracture appearance (Fig. 2b) would reflect an intermediate toughness condition. As expected, flat, brittle fracture was observed at low temperatures and the fracture surfaces appeared to be less rough. On the contrary, at higher temperatures, slant ductile fracture was observed. The amplitude and slope of surface hillocks were then large, which means the surface roughness is higher.

4.3. Fracture dimension and impact toughness

The linear fractal dimension, D_L, was determined from the data of the perimeters of the islands and their enclosed areas, measured by the digital image analysis system. The magnification and the digital image pad resolution (set at 333 μm) determine the ruler length, and three ruler lengths, 6.66, 0.666 and 0.2664 μm, were chosen at the magnifications of $\times 50$, $\times 500$ and $\times 1250$, respectively.

Shown in Fig. 3 are the "islands" of a fracture surface at different levels. Note that over a sequence of the polished levels, new "islands" appear at level 6. The value of D_L was then determined using a log–log plot of area versus perimeter measured at different levels. A typical example is shown in Fig. 4. The values of fractal dimensions at different ruler lengths are given in Table II. Fig. 5a–c illustrate the relationships between the fractal dimension, D_L, and the impact toughness, E. If the ruler length is large (6.66 μm), the impact energy appears to decrease with increasing D_L. If the ruler length is small (0.666 μm and 0.2664 μm), E decreases as D_L increases. This result is consistent with the work of Lung and Mu [8]. The positive

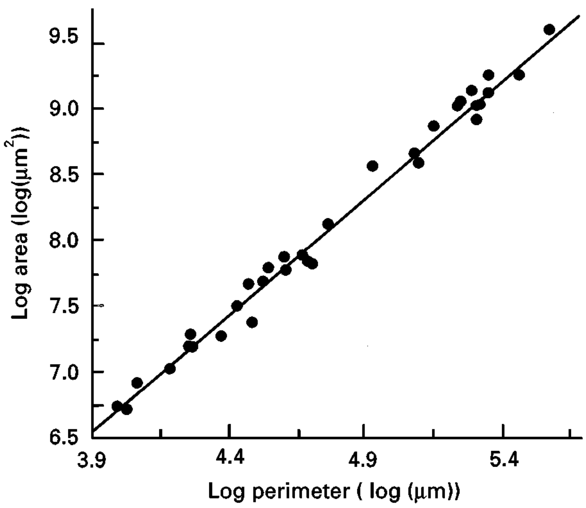

Figure 4 A typical plot of log (area) versus log (perimeter). The linear fractal dimension, D_L, is determined from the slope of the straight line ($D_L = 2$/slope).

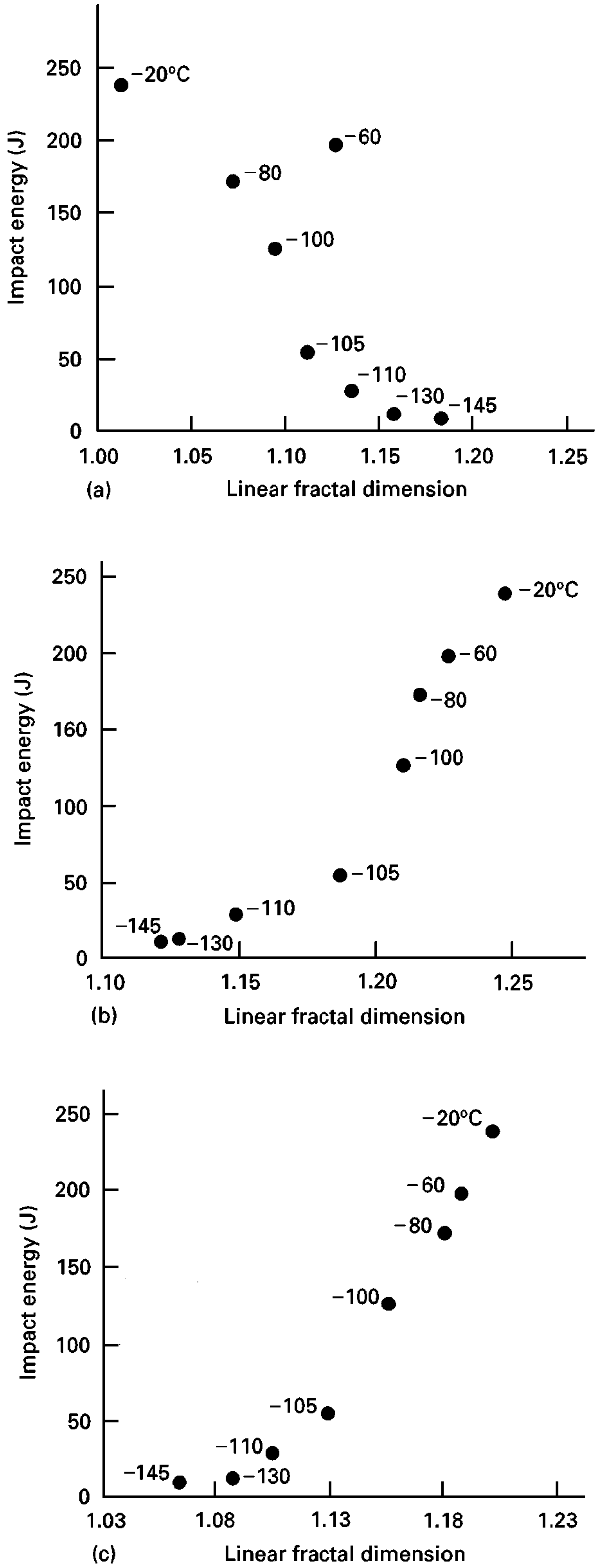

Figure 5 Impact energy versus linear fractal dimension. (a) Ruler length = 6.66 μm. Note that the measurement at −60 °C involved error. (b) Ruler length = 0.666 μm. (c) Ruler length = 0.2664 μm.

relationship between D_L and E is easy to understand, i.e. the higher the D_L value, the rougher is the surface and the tougher is the material.

In addition, the slopes measured in $\ln E$ versus D_L plots with the 0.666 and 0.2664 μm (Fig. 6) rulers are very close, indicating that the D_L value measured with the 0.2664 μm ruler is practically reaching the

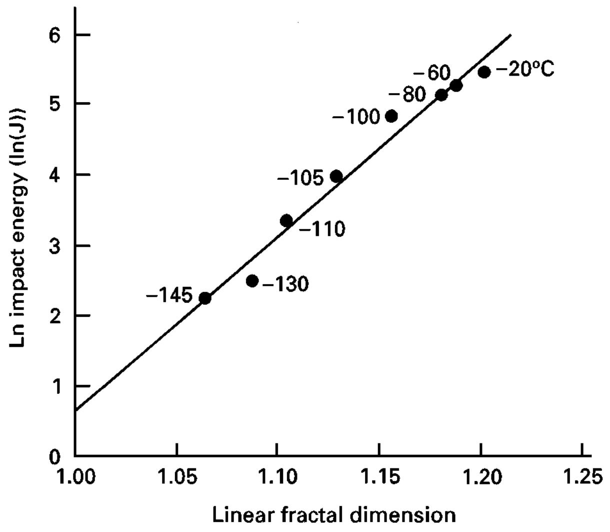

Figure 6 Plot of ln(impact energy) versus linear fractal dimension at ruler length = 0.2664 μm.

true value. Using least-square fitting, we have

$$E = E_0 e^{25D'} \tag{3}$$

where $E_0 = 1.9$ J representing the impact toughness in Euclidean space, D' is the fractal dimensional increment, defined by $D' = D_S - 2 = D_L - 1$, and D_S refers to the surface fractal dimension. Despite the scatter of the data, Equation 3 is useful as an empirical relationship to which the results of future studies on high-strength low-alloy (HSLA) steels can be quantitatively compared. And when further experimental data are available and consistent, fractal dimension may then be acceptable as a new material parameter for the fracture process.

5. Conclusion

The fracture surfaces of a high-strength low-alloy steel (ASTM A710) were shown to be fractals. With ruler lengths of 0.666 μm or less, the fractal dimension was proportional to the fracture toughness. With a ruler length of 6.66 μm, the relationship was reversed and unrealistic.

For A710 steels, the linear fractal dimension, D_L, increases as the fracture toughness, E, increases. They are related by the empirical equation, $E = E_0 e^{25D'}$, where $E_0 = 1.9$ J representing the impact toughness in Euclidean space, and D' is the fractal dimensional increment, defined by $D' = D_S - 2 = D_L - 1$.

Acknowledgements

We thank Dr W. F. Qin, Dr E. J. Kaufmann and Professor D. A. Thomas, Lehigh University, for helpful discussions. The work was partially supported by the NSF Engineering Research Center, Advanced Technology for Large Structural Systems (ATLSS), at Lehigh University.

References

1. B. B. MANDELBROT, D. E. PASSOJA and A. J. PAULLAY, *Nature* **308** (1984) 721.
2. B. B. MANDELBROT, "The Fractal Geometry of Nature" (Freeman, New York, NY, 1982), p. 109.
3. J. J. MECHOLSKY and T. J. MACKIN, *J. Mater. Sci. Lett.* **7** (1988) 1145.
4. J. J. MECHOLSKY, D. E. PASSOJA and K. S. FEINBERG-RINGEL, *J. Amer. Ceram. Soc.* **72** (1989) 60.
5. C. T. CHEN and J. RUNT, *Polym. Commun.* **30** (1989) 334.
6. C. S. PANDE, L. E. RICHARD, N. LOUAT, B. D. DEMPSEY and A. J. SCHWOEBLE, *Acta Metall.* **35** (1987) 1633.
7. Z. Q. MU and C. W. LUNG, *Phys. D Appl. Phys.* **21** (1988) 848.
8. C. W. LUNG and Z. Q. MU, *Phys. Rev. B* **38** (1988) 11781.
9. C. W. LUNG and S. Z. ZHANG, *Physica D* **38** (1989) 242.
10. R. J. JESSEMAN and G. C. SCHMID, *Weld. J.* **62** (1983) 321s.
11. T. W. MONTEMARANO, B. P. SACK, J. P. GUDAS, M. G. VASSILAROS and H. H. VANDERVELDT, *J. Ship Production* **2** (1986) 145.
12. T. L. ANDERSON, J. A. HYATT and J. C. WEST, *Weld. J.* **66** (1987) 21.
13. A. D. WILSON, E. G. HAMBURG, D. J. COLVIN, S. W. THOMPSON and G. KRAUSS, in "Proceedings of Microalloying '88" (ASM International Press, Metals Park, OH, 1988) p. 259.
14. W. BOLLIGER, R. VARUGHESE, E. KAUFMANN, W. F. QIN, A. W. PENSE and R. S. STOUT, *ibid.*, p. 277.
15. M. COSTIN and J. L. CHERMANT, *Int. Metall. Rev.* **28** (1983) 228.
16. J. J. FRIEL and C. S. PANDE, *J. Mater. Res.* **8** (1993) 100.

Received 6 September 1996
and accepted 13 February 1998